Simulations and Observations of Cloudtop Processes

S. T. Siems*, C. S. Bretherton*, and M. B. Baker**
*Applied Mathematics Department **Geophysics Program
University of Washington
Seattle WA 98195

Turbulent entrainment at zero mean shear stratified interfaces has been studied extensively in the laboratory and theoretically for the classical situation in which density is a passive tracer of the mixing and the turbulent motions producing the entrainment are directed toward the interface (see Turner, 1986, for a comprehensive review). For gases at high Reynolds number, the entrainment velocity w_e at the interface separating a lower turbulent fluid of mean virtual potential temperature $\overline{\theta_v}$ from a nonturbulent fluid of virtual potential temperature $\overline{\theta_v}-\Delta\theta_v$ depends only on a Richardson's number, which can be defined as

$$Ri \equiv \frac{g\Delta\theta_v h}{w^2\overline{\theta_v}} \tag{1.1}$$

where w and h are turbulent velocity and length scales. Carruthers and Hunt (1986), Linden (1973), Stull (1976), and others have described the entrainment mechanism at intermediate Ri in terms of eddies impinging on the interface and dragging down wisps of upper layer fluid. Lidar pictures (Atlas et al., 1986) show evidence of dome-wisp like entrainment in the inversion topping the dry atmospheric boundary layer.

In the layer cloud situation, radiative and evaporative cooling tend to drive convective motions away from the interface, instead of toward it as in the classical flows. Moreover, the function $\theta_v(F)$ is piecewise linear in the cloud case, where F is the fraction of cloudy air in a parcel formed by mixing cloud and upper air. This behavior introduces another parameter into the problem, which we define as D_*:

$$D_* \equiv \frac{\Delta_*}{\Delta\theta_v F_*} \tag{1.2}$$

where $\Delta_* \equiv \theta_v(F_*) - \overline{\theta_v}$ and F_* is the mixing fraction of exactly saturated air.

The effects of these properties of the cloud-clear interface on the entrainment process are not well understood. Observations (Nicholls and Leighton, 1986; Caughey et al., 1985) in stratocumulus show that evaporative cooling enhances entrainment over that expected in the dry, linearly mixing case, even if $D_* > 0$. On the other hand, observations (for example, Hanson, 1984) show that even in cases for which the "cloudtop entrainment instability," or CEI, criterion holds ($D_* < 0.0$), clouds do not necessarily thin or breakup, as had been suggested by Deardorff (1980), Randall (1980) and others. This suggests that kinetic energy due to evaporative cooling is a secondary effect in determining cloudtop motions in these cases.

It has been suggested (Caughey et al., 1985; Nicholls and Leighton, 1986) that detachment of small, cooled parcels from the base of the optically active layer below cloudtop gives rise to convective circulations which result in turbulent motions at cloudtop and thus in turbulent entrainment. Mahrt and Paumier (1982) showed that, in the case of some mean shear at cloudtop, mixing of cloud and clear air was in the main confined to the downwind side of penetrative cloudy elements. They found significant heat fluxes carried by non-cloudy, yet mixed, air parcels.

It is the purpose of our numerical simulations and data analysis to investigate these processes and, specifically, to focus on the following questions.

(1) Can local cooling below cloudtop play an important role in (a) setting up convective circulations within the cloud, and (b) bringing about entrainment?

(2) Can CEI alone lead to runaway entrainment under geophysically realistic conditions?

(3) What are the important mechanisms of entrainment at cloudtop under zero or low mean shear conditions?

II. Numerical Simulations

We have numerically simulated the stratocumulus inversion layer by a two-dimensional fluid dynamic representation of a Boussinesq layer. We use the following set of governing equations:

$$\frac{\partial \zeta}{\partial t} = -(\vec{U}\cdot\nabla)\zeta + \nu\nabla^2\zeta - b_x \tag{2.1}$$

$$\zeta = \nabla^2\Psi \tag{2.2}$$

$$\vec{U} = (-\partial\Psi/\partial z, \partial\Psi/\partial x) \tag{2.3}$$

$$b = f(\gamma_1, \gamma_2) \tag{2.4}$$

$$\frac{\partial \gamma}{\partial t} = -(\vec{U}\cdot\nabla)\gamma + \nu\nabla^2\gamma \tag{2.5}$$

where ζ is the vorticity, Ψ is the stream function, $\vec{U}$ is the velocity, ν is an eddy diffusivity, and b is the buoyancy, which is a linear function of the two conserved quantities γ_1, γ_2 (the equivalent potential temperature and total water content or saturation point temperature and pressure (Betts, 1982; Bretherton, 1987)). These equations are solved with a finite differencing scheme in time and space. Periodic boundary conditions are assumed in x and Dirichlet boundary conditions in z. The two-layer stratified fluid is initially at rest, and at t = 0 we apply a small perturbation in the conserved variables. This stratified flow would remain stable without the incorporation of additional physics to the model. We discuss here simulations in which evaporative cooling drives the circulations. Note that all mixing, turbulent and diffusive, is represented by the eddy diffusivity term $\nu\nabla^2$. Values used here are orders of magnitude larger than values appropriate for thermal and molecular diffusion. Stability considerations prevented use of lower values; thus the simulated flow is laminar rather than turbulent. While the upper boundary did not appear to have an important effect, the lower boundary forced an artificial circulation in the fluid and gave rise to spurious fluxes of the conserved quantities.

Figure 1 displays $\theta_v(F)$ for three cases: namely, the measurements discussed below and two situations we have simulated. Preliminary results of our simulations are shown in Figures 2 and 3. In the right hand figure of each pair, we show contours of a variable which is proportional to the difference between the saturation point pressure (Betts, 1982) and the actual pressure; thus the zero contour indicates cloudtop and the most dense mixtures of the upper and lower fluids. The area below this contour represents the cloud; small contour values represent mixtures which are close to saturation and, therefore, relatively dense. The left hand figure of each pair shows the stream function. Initially, the inversion layer is at height 1, and the fluid is at rest. The simulations represent the situation at later times, when the circulations are established.

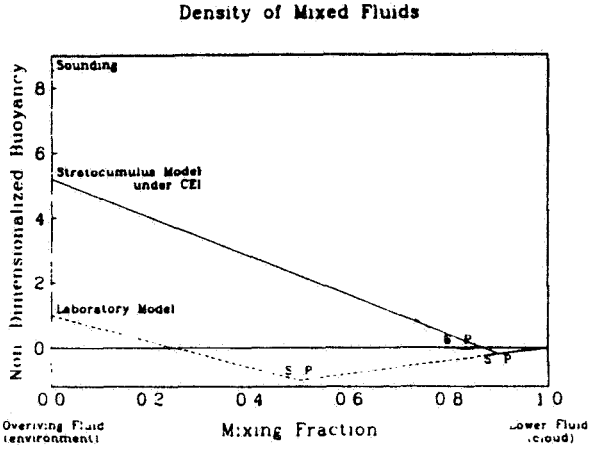

Figure 1. $\theta_v(F)$, where F is the fraction of cloudbase air in a mixture of cloudbase and upper level air. Solid and dashed lines: numerical simulations (see text); dotted line: computed from 19:06 sounding, July 5, 1987.

Figure 2 shows a geophysically realistic case (solid curve, Figure 1; $D_* = -0.04$.) The initial cooling at cloudtop has led to the formation of a steady circulation within the moist, cool cloud, indicating that evaporative cooling is a significant source of turbulent kinetic energy. The dry, lighter, inversion fluid is affected only by diffusion. The circulation produces "cool pools" of unsaturated air of approximately the same buoyancy as the cloud. Penetrative plumes with high evaporation rates form under these pools. A sharp interface between layers was maintained by the circulation, instead of the gradient layer predicted by Turner and Yang (1963). Under these physically reasonable initial conditions satisfying the CEI condition, no indication of runaway entrainment evolves.

Figure 3 corresponds to a laboratory simulation (Shy and Breidenthal, personal communication) in which CEI is a greater effect (dashed curve, Figure 1; $D_* = -2.$). Under these extreme conditions runaway entrainment occurs. The contamination of the lower fluid with the newly created mixed fluid becomes important before a semi-steady circulation is established.

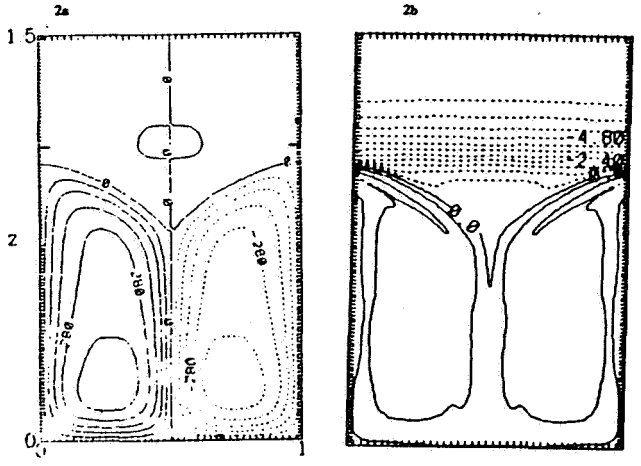

Figure 2. Vertical cross section of simulated stratocumulus deck $D_* = -.04$, at a time when steady circulation has developed. a) Stream function. b) Negative values of the contoured variable correspond to positive buoyancy: zero contour is cloudtop.

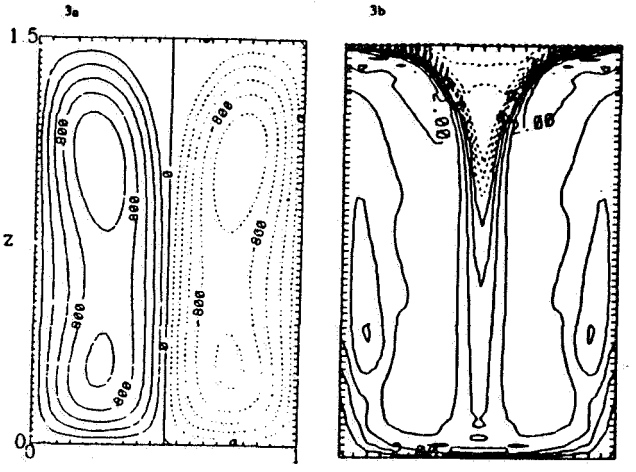

Figure 3. As in Figure 2, but for "laboratory" sounding, $D_* = -2.0$.

III. Data Analysis

We report here on a preliminary analysis of high resolution measurements made aboard the NCAR Electra on July 5, 1987, as part of the FIRE project. For averaged 1-Hz thermodynamic measurements we used the static (fuselage) pressure, temperature measured by the the Rosemount thermometer, liquid water from the Johnson-Williams device, and vapor content computed by averaging, filtering and applying a 2-second lag (Austin, personal communication) to the signal from the dewpoint sensors, and we used the 20 Hz FSSP and Lyman α records as high resolution tracers of the presence of cloud and pockets of moistened air.

Figure 4 displays the sounding made at 19:06-19:10 GMT in saturation point coordinates (Betts, 1982), showing the thermodynamic structure of the cloud and above cloud layers. The mixing line lies close to a θ_v isopleth. There was some mean shear within the layer, permitting the identification of air parcel origin by horizontal velocity, as well as thermodynamic properties. The sounding values at 950 and 910 mb were used to calculate the dotted curve in Figure 1. The CEI criterion is marginally met; $D_* = -.006$ and the cloud was quite solid.

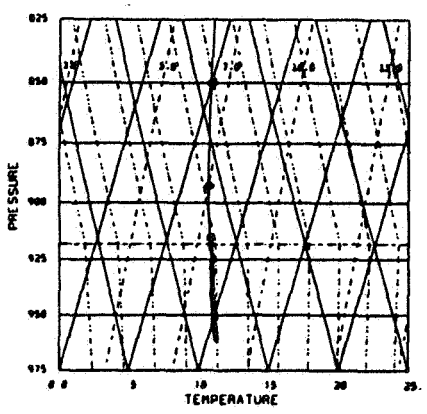

Figure 4. 19:06-19:10 GMT, July 5 sounding computed in saturation point coordinates. Dotted lines are θ_v isopleths computed at cloudtop, 920 mb.

Figure 5 shows portions of the time series of liquid water, w, θ_v and the buoyancy flux (calculated as the simple covariance, unfiltered, of w and θ_v) over an in-cloud segment at about 936 mb. The cloud was highly turbulent and the most notable features of the traces are the distinct events, tens of meters in scale, at intervals of about 4-5 kilometers in which the liquid water decreased sharply and there were large excursions in vertical velocity. This is the scale of the major undulations in cloudtop shown by lidar measurements later on this flight. Examination of the radiative fluxes and vapor content (not shown) suggests that the events were passage through columns of clear, and in some cases unsaturated, air. Note the highly intermittent character of the buoyant fluxes; convection is driven from below as well as from the top, and the breaks between cloud segments appear to play an important dynamic role.

Cloudtop rose before the cloudtop traverse, a segment of which is shown in Figure 6. The aircraft flew in and out of cloudy segments at about 912 mb. The cloudy segments, which were more turbulent than the intervening clear air but much less turbulent than the cloud at lower levels, consist of regions of high liquid water content, separated by shorter, more dilute regions referred to by Mahrt and Paumier as "wisps." Note the high turbulence levels marking small turbules of cloudy air and the high vapor content in some of the "wisps." Mixing appears fairly localized to the edges of the cloudy segments, as evidenced by the spikes in horizontal and vertical velocity there. Evaporative cooling is probably responsible for the velocity spikes at these interfaces. The spatial scales of these mixing regions are comparable with the scales of the liquid-free regions seen at lower levels, but the cooling is not sufficient to explain the descent of cloudtop air to the lower level without some dynamic forcing. The nonturbulent air between the cloudy segments is the result of prior mixing of cloud and upper level air, and may represent evidence of "cool pools" as shown in the calculations. (See Fig. 2).

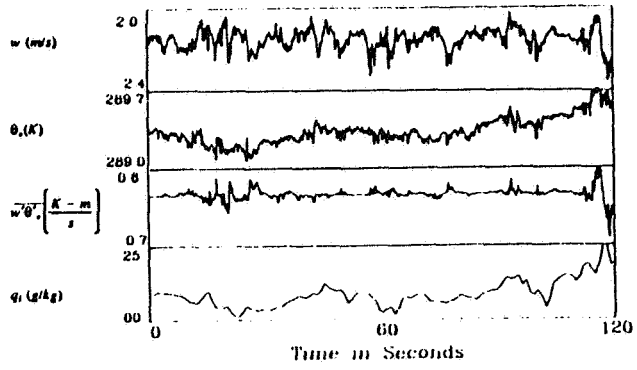

Figure 5. In-cloud measurements made at 936 mb, 18:40-18:45 GMT, Average aircraft velocity about 105 m/s. See text.

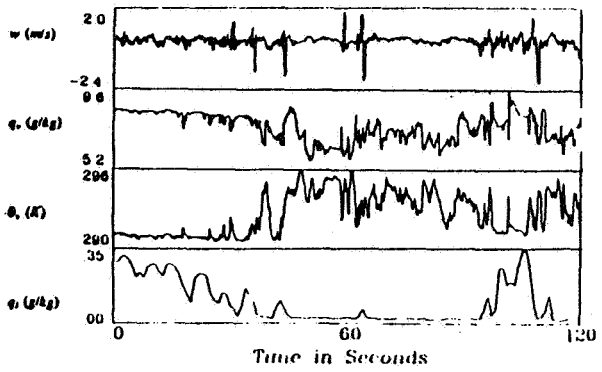

Figure 6. Cloudtop measurements made at 912 mb, 19:20-19:25 GMT. See text.

IV. Discussion

From these preliminary results, it appears that mixing of cloudy and clear air takes place primarily in highly localized regions, both at the edges of large cloudy segments, and in the vicinity of small cloudy turbules rising into the cloudtop region. The descent of the mixed air is apparently accelerated by evaporative cooling. However, our simulations, as well as the observations, show that relatively quiescent, mixed, clear air accumulates between the upward penetrating cloud elements, and they suggest that it is not sufficiently negatively buoyant to be efficiently drawn down into the cloud. Moreover, it appears from the simulations that, under physically realistic conditions, evaporative cooling alone does not lead to runaway entrainment, even when the CEI criterion is met, unless D_* is a very large negative number.

The relatively low efficiency of evaporative cooling in generating turbulent kinetic energy at the interface may be due partially to the fact that $\theta_v(F) < \theta_v(1)$ only for relatively high F values. Parcels with these mixture ratios are probably characteristic only of air at the base of the inversion layer. The displacement of the acceleration due to evaporative cooling from the upper layer fluid, and thus from the region at which it could most efficiently promote entrainment, is further suggested by recent laboratory experiments (Johari, 1988), showing that no molecular mixing occurs in a buoyant (or in this case, negatively buoyant) thermal until it has moved a distance comparable to its diameter. The evaporatively cooled parcels seen at cloudtop have dimensions on the order of tens of meters, so they may be roughly that far from their first encounter with upper level fluid before they receive the additional downward acceleration due to the evaporation. For small D_*, the mixed fluid simply accumulates at cloudtop, reshaping the density profile and thus slightly facilitating further entrainment there.

Acknowledgement: This research was supported by NSF grant ATM-8620165.

References

Atlas, D., B. Walter, S. Chou and P. Sheu (1986), *J. Atmos. Sci. 43*, 1301-1317.
Betts, A. (1982), *J. Atmos. Sci. 39*, 1484-1505.
Bretherton, C. (1987), *J. Atmos. Sci. 44*, 1869-1874.
Carruthers, D. and J. Hunt (1986), *J. Fluid Mech. 165*, 475-502.
Caughey, S., B. Crease, and W. Roach, (1982), *Q. J. Roy. Met. Soc. 108*, 125-144.
Deardorff, J. (1976), *Q. J. Roy. Met. Soc. 102*, 563-582.
Deardorff, G. (1980), *J. Atmos. Sci. 37*, 131-147.
Hanson, H. (1984), *J. Atmos. Sci. 41*, 1226-1234.
Johari, H. (1988), AMS Conference on Turbulence and Diffusion.
Linden, P. (1973), *J. Fluid Mech. 60*, 467-480.
Mahrt, L. and J. Paumier (1982), *J. Atmos. Sci. 39*, 622-634.
Nicholls, S. and J. Leighton (1986), *Q. J. Roy. Met. Soc. 112*, 431-460.
Nicholls, S. and J. Turton (1986), *Q. J. Roy. Met. Soc. 112*, 461-480.
Randall, D. (1980), *J. Atmos. Sci. 37*, 125-130.
Rogers, D. and J. Telford (1986), *J. Atmos. Sci. 37*, 481-500.
Stull, R. (1976), *J. Atmos. Sci. 33*, 1260-1267.
Turner, J. S. (1986), *J. Fl. Mech. 173*, 431-471.
Turner, J. and I. Yang (1963), *J. Fluid Mech. 17*, 212-224.